



The Dispersion Energy Parameters, Linear and Nonlinear Optical Properties of Transparent Mn:ZnO Nanolayers

Cihat Aydin 

¹Mersin University, Faculty of Engineering, Metallurgy and Materials Engineering Department, Mersin, Turkey

Abstract

Throughout this research, the impact of Manganese doping on the optical characteristics of ZnO nanolayers was explained. The sol-gel spin coating technique has significant advantages due to the mixing of components on the atomic scale and provides excellent control over the composition that was employed to produce samples. The optical characteristics of Mn: ZnO nanolayers, were determined with the help of UV-VIS-NIR spectroscopy. The linear and nonlinear optical properties of nanolayers were investigated between 300 and 800 nm wavelengths. The dispersion properties of the samples were determined and interpreted in accordance with the single-oscillator model. The third-order nonlinear optical characteristics indicate a good correlation between theoretical and experimental results. These interesting results obtained by Mn-doping of ZnO showed a significant behavior for technological applications in electronic, optoelectronic devices and nonlinear optical applications.

Keywords: Nonlinear optics, Opto-electrical properties, dispersion energy parameters, optical band gap

1. INTRODUCTION

Due to their unique properties, optical thin films have been widely used in the automotive industry, medical equipment, communication, computers, optoelectronics, spintronics, biomaterials, energy conversion, data storage, and even architecture [1]. ZnO draws great interest as a transparent conductive material because of its high optical transparency in the visible light region [2]. Therefore, ZnO is a suitable material for electronic and optical devices [3]. Furthermore, ZnO offers unique photocatalytic properties[4].

Bandwidth engineering research has been recently accelerated to improve the characteristics of semiconductors with wide bandwidths [5]. Therefore, comprehensive research has been conducted for the purpose of changing the characteristics of zinc oxide for various applications [6]. Developments in the synthesis of high-quality ZnO nanostructures allow the production of semiconductors, especially those used in nanoscale device applications [7]. The production of new semiconductors has been renovated with the development of semiconductor devices in science and industry.

In the present research, nanostructured doped and pure ZnO films produced by the spin coating technique. Also, the variation of linear and nonlinear optical properties by the Mn doping concentrations of ZnO nanolayers thin films were studied.

2. 2. EXPERIMENTALS

In this study, All chemicals were provided by Merck and analytical purity was protected. The solutions were quantified as 0.5 M, 5 ml, and the contents were put into test tubes containing solvent (2-methoxyethanol). These solutions were stirred at room temperature using a magnetic stirrer and an ultrasonic stirrer. Stirring was repeated under the same conditions after the dopant source was added. Finally, the stabilizer (Monoethanolamine) was added and stirring was repeated under the same conditions. Stirring was carried out in a magnetic stirrer (2h at 60 °C) to obtain a homogeneous gel from the solution. The microscope glasses were respectively ultrasonic cleaned in ethyl alcohol, acetone and pure water for 15 minutes and completely with the help of nitrogen gas. The growth of thin films was accomplished with the help of a spin coating devices(1500 rpm, 20 seconds). For drying, the substrates were held on a heater pre-set to 150 °C for 10 minutes. In the final step, the obtained films were heat-treated at 550 °C for 2 hour. Care was taken to prepare thin films under the same conditions for all doping ratios. Absorption $T(\lambda)$, reflectance $R(\lambda)$ and permeability $A(\lambda)$ measurements of the prepared nanolayers were obtained with a spectrophotometer (Shimadzu UV-VIS-NIR 3600) in the wavelength range of 300 nm-800 nm. All measurements were made at room temperature.

* Corresponding author
Email: cihataydin@mersin.edu.tr



3. RESULTS AND DISCUSSION

3.1. 3.2. Optical properties of pure and Mn-doped ZnO nanostructured films

The change in the absorption properties of pure and Mn-doped ZnO film samples at room temperature is shown in Fig.1. Upon examining Fig. 1, it is possible to say that the specific absorption properties of ZnO are significantly affected by Mn-doping. All samples have the ultraviolet absorption edges ranging from 300 - 400 nm. Depending on the Mn-doping ratio, the absorption value also increased. This increase is thought to have resulted from further absorption of photons because of the introduction of Mn-defects into the forbidden band [8,9]. The absorption spectrum of pure and Mn-doped ZnO thin films showed strong absorption properties in the wavelengths of 400 nm and lower, and a continuous increase in absorption was determined. However, absorption reaches an equilibrium value since the samples exhibit permeability in the wavelengths ranges equal to or greater than 400 nm [10,11]. The possible reason for the sharp absorption peak at about 300 nm for the samples may be the photostimulation of electrons from the valence band to the conduction band [12,13,14]. With Mn-doping, this absorption edge shifts to higher wavelengths. It is noteworthy that the pure ZnO sample has the lowest absorbance in the visible spectrum range because it is receiving high-energy photons, causing the activation of *sp-d* exchange interactions and typical *d-d* transitions [15]. This has been similarly stated in previous research [16].

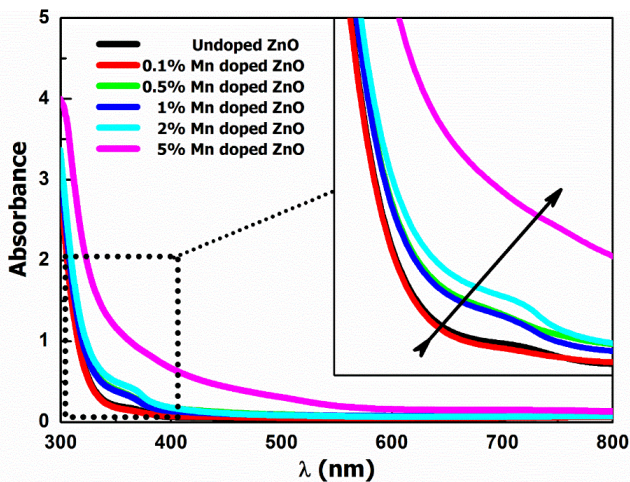


Figure 1. Absorbance spectra of the Mn: ZnO nanolayers

Fig. 2 demonstrates the reflection spectra of pure and Mn-doped ZnO nanolayers. As observed in Fig. 6, the reflection curves of the nanolayers demonstrated a peak in the wavelength of about 390 nm. The peak in question changes according to Mn-doping. This proves that the forbidden energy ranges of films vary with Mn-doping. This Mn doping leads to reduce the reflection values of the nanolayers compared to the pure ZnO film sample. The reduction of reflection by Mn-doping has been previously reported and such detail is in well agreement with our result [17]. The possible reason for the alteration in optical reflection can be

the morphological alteration in films since the aspect ratio of crystallites changes according to the film thickness. This has been similarly stated for ZnO thin layers produced using several deposition routes[18]. Moreover, an increase occurred in the reflection values as they shifted to short wavelengths. This can be attributed to the back reflection of photons as a result of their higher interaction with electrons, atoms, or crystal molecules due to their increased energy.

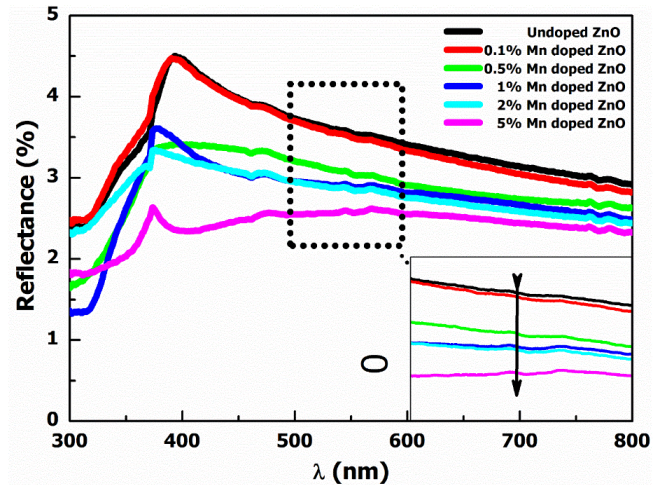


Figure 2. Reflectance spectra of the Mn: ZnO transparent nanolayers

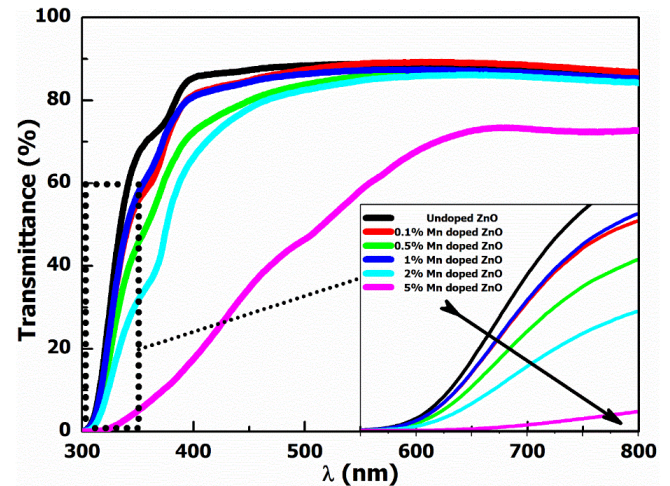


Figure 3. Transmittance spectra of the Mn: ZnO transparent nanolayers

The optical transmission spectra of pure and Mn-doped ZnO films that were recorded in the wavelength range of 300-800 nm are presented in Fig. 3. The prepared samples demonstrate high transparency in the visible range, and the transmission values decrease because of Mn-doping in all samples. The reduction in optical transmission is associated with the light loss caused by the structural properties of films, oxygen gaps, and dispersion in the grain boundaries [19] because the transmission of films, in general, depends on the surface morphology and structure [20]. The main cause of the loss of transmission observed due to increased Mn-contents in ZnO thin films may be deterioration of crystal quality of samples, increase in the defect density with the increasing doping ratio [21], and the presence of dispersion centers [22]. As the Mn-ratio increased, the transmission decreased as the optical dispersions increased. The trans-

mission spectrum of the thin films presented in Fig. 3 shows a sharp absorption edge in the wavelength range of 300-350 nm. This band edge shifts towards high wavelengths in parallel with increasing Mn- concentrations. This proves the successful incorporation of Mn-ions into the ZnO matrix. The possible reason for this is the low UV light absorption due to the increasing Mn-ratio [23]. This has been confirmed by similar results from many studies in the literature on doped and pure ZnO thin films [24].

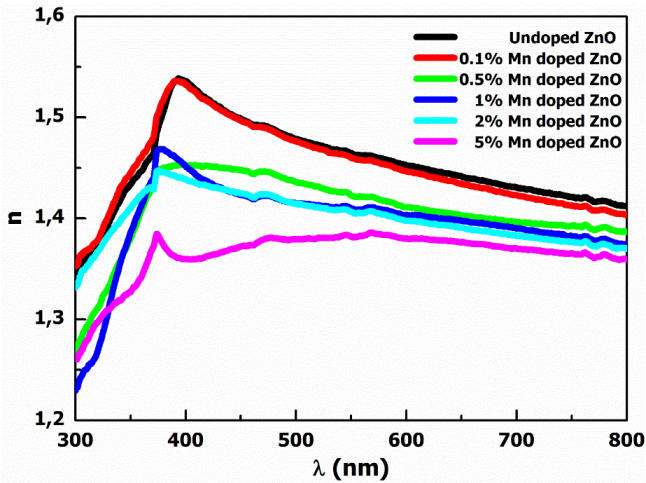


Figure 4. *n* (Refractive index) spectra of Mn:ZnO nanolayers

Finding the refractive index of semiconductor materials takes a significant part in identifying the suitable usage area by taking advantage of the optical characteristics of the material. In the design of the device, the refractive index represents the key parameter in the integrated optical devices, including switches, modulators, filters, etc. The refractive index can be adapted to any value that is needed for use in filters through the doping concentrations. The *n* and *k* values of the nanostructured thin films generated with the sol-gel technique were found from the transmittance and reflectance spectra.

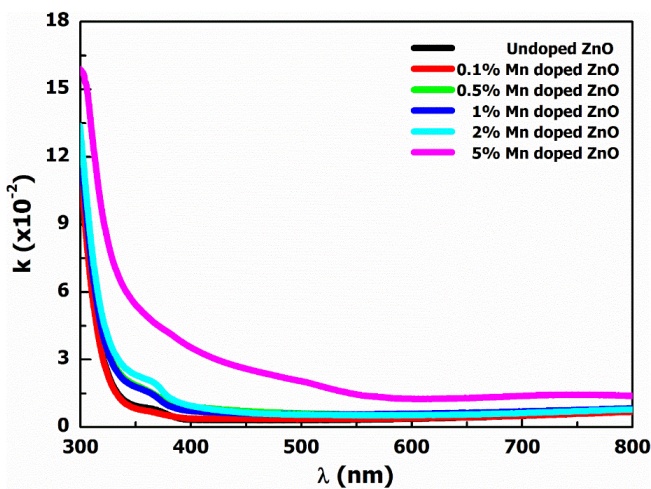


Figure 5. *k* (Absorption index) spectra of Mn:ZnO nanolayers

Refractive index and absorption index values of produced nanolayers by Sol-Gel technique were found with the help of transmission and reflection curves.

In accordance with the analysis introduced by Moss, the absorption coefficient α was calculated from the measurements of $T(\lambda)$ and $R(\lambda)$ using the equation presented below [9]:

$$T = \frac{[(1-R)^2 \exp(-\alpha d)]}{[(1-R)^2 \exp(-2\alpha d)]} \tag{1}$$

$$R = \frac{(n-1)^2 + k^2}{(n+1)^2 + k^2} \tag{2}$$

It is possible to analyze these spectra for the purpose of determining optical constants, including refractive index (*n*) and damping coefficient (*k*). The correlation below can represent the complex refractive index of ZnO-based thin films [9]:

$$\tilde{n} = n(\lambda) + ik(\lambda) \tag{3}$$

where *n* refers to the real part, and *k* refers to the imaginary part of the complex refractive index. With the help of the reflection values of Mn: ZnO thin film samples, the refractive index (*n*) is computed by the following formula that is called Fresnel's formula [10]:

$$n = \frac{(1+R)\sqrt{4R - (1-R)^2 k^2}}{1-R} \tag{4}$$

It is possible to use the formula presented below for the purpose of obtaining the absorption index (*k*) [11]:

$$k = \frac{\alpha \lambda}{4\pi} \tag{5}$$

where λ is the wavelength and α is the absorption coefficient. The change in the *n* and *k* values can be calculated by using Fresnel's equations against wavelengths are demonstrated in Fig. 4 and Fig. 5, respectively. As can be observed from Fig. 4, with generally increasing incident wavelength, the refractive index value first increased and then decreased. The pure ZnO sample showed the highest refractive index. A non-linear decrease is observed in the refractive index values with Mn-doping in the ZnO matrix. The refractive index comprises two regions for all studied samples. The first one is lower wavelengths (abnormal dispersion) where an increase occurs in the refractive index with increasing wavelength, and the second one is the region where a decrease occurs in the refractive index (normal dispersion) with an increase in wavelength [9]. This abnormal dispersion determined in the refractive index in the lower wavelength region is due to the resonance impact between electromagnetic radiation and electron polarization by adding Mn-ions into the ZnO structure [13], which in turn causes the binding of electrons to the oscillating electric field. Likewise, it is possible to explain the decreasing tendency in higher wavelengths by the effect of band levels. Gradually decreasing *n* and *k* values result from increasing carrier concentrations as a consequence of changing the chemical composition of samples by doping. The findings in question have been similarly stated for ZnO nanomaterials [25]. The refractive index (*n*) of the undoped and Mn-doped ZnO nanostructured thin films at different wavelength are demonstrated in Table 1.

Table 1. *n* (Refractive index) of the Mn: ZnO nanolayers at different wavelength

Samples	The refractive index (<i>n</i>)		
	at 300 nm	500 at nm	700 at nm
Pure ZnO	1,3472	1,4787	1,4306
0.1% Mn doped ZnO	1,3545	1,4763	1,4229
0.5 % Mn doped ZnO	1,2646	1,4360	1,3966
1 % Mn doped ZnO	1,2295	1,4152	1,3901
2 % Mn doped ZnO	1,3319	1,4146	1,3826
5 % Mn doped ZnO	1,2616	1,3793	1,3702

The forbidden energy gap of the semiconductor thin films generated was found from the $(\alpha h\nu)^2-h\nu$ graph by utilizing the basic absorption spectrum. The energy gap value of the point at which the linear section of the mentioned change intersects the $h\nu$ axis at $(\alpha h\nu)^2 = 0$ gives the forbidden energy band gap of the studied semiconductor. The formula presented below and known as Tauc's equation was utilized to calculate the forbidden energy band gap as follows [26]:

$$(\alpha h\nu)^2 = A(h\nu - E_g) \tag{6}$$

where α refers to the absorption coefficient, $h\nu$ refers to the photon energy, E_g refers to the forbidden bandgap, and A refers to the constant. The $(\alpha h\nu)^2-h\nu$ plots to determine the forbidden energy gap of pure/Mn-doped nanostructured ZnO thin films are demonstrated in Fig. 6.

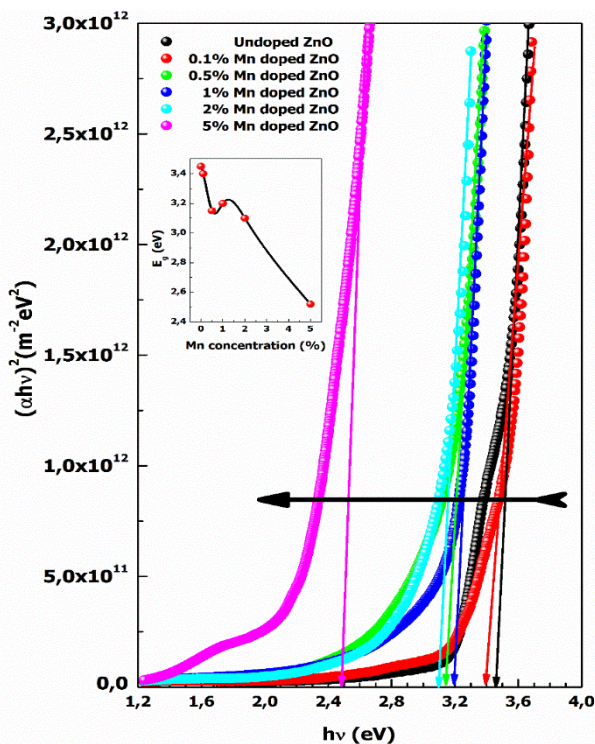


Figure 6. Tauc's plots of the Mn: ZnO nanolayers

With the help of these curves, the forbidden energy gaps (E_g) of the understudied samples were calculated and are presented in Table 2. The change in the energy gap with Mn-concentrations is given in Fig. 6. It is observed that the highest value of the energy gap belongs to the pure ZnO sample and the lowest value belongs to 5% Mn-doped ZnO film sample. The obtained findings on the energy gap are in compliance with the bulk ZnO (3.37 eV) [10] and ZnO samples gen-

rated by similar methods in the literature [27]. The energy gap of the samples generally decreased with the increasing Mn-ratio. There may be two reasons for the decreasing optical band gaps of Mn-doped ZnO thin films. In other words, there is an inverse proportion of the forbidden energy gap to the size change because the size of doped Mn-grains is much smaller than the excitonic Bohr's radius in ZnO. Substituting both Mn-atoms and Mn- in the interstitial position with Zn-can lead to a lattice distortion [3]. Therefore, structural distortion and irregularity in the ZnO lattice may produce a change in the optical bandgap of Mn-doped ZnO films. Since the optical band gap is associated with the lattice constant [28], the latter may be attributed to the modification of the band structure due to the exchange interactions between sp-d electrons in ZnO [29]. This type of change interaction is caused by the reinforcement that causes the bandgap to be reduced by decreasing the bottom of the conduction band and increasing the top of the valence band . The narrowing of the ZnO bandgap with doping has been observed in a similar way in the previous research [30],[31],[32].

Table 2. Optical band gap of present work on ZnO nanolayers

	E_g (eV)
Pure ZnO	3.45
0.1% Mn doped ZnO	3.40
0.5 % Mn doped ZnO	3.15
1 % Mn doped ZnO	3.20
2 % Mn doped ZnO	3.10
5 % Mn doped ZnO	2.52

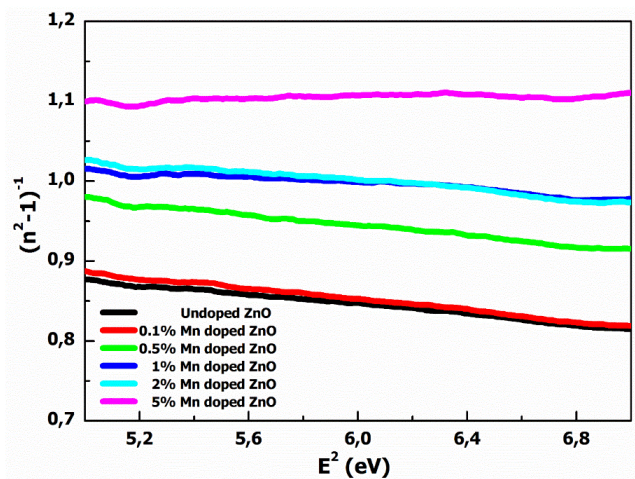


Figure 7. Plots of $(n^2-1)^{-1} - (h\nu)^2$ of the Mn: ZnO nanolayers.

Refractive dispersion takes a significant part in investigating the optical properties of materials since it represents an essential factor for designing devices that will be utilized for image distribution in optical communications. The refractive index distribution of the nanostructured thin films acquired in the current research was studied by the Wemple-DiDomenico (WD) model. The dispersion theory is expressed by the following equation in accordance with the effective single-oscillator model of the refractive index (n) in the low absorption region [34]:

$$n^2 = 1 + \frac{E_d E_0}{E_0^2 - (h\nu)^2} \tag{7}$$

where n denotes the refractive index, E_o denotes the single oscillator energy for electronic transitions, E_d denotes the dispersion energy for interband optical transitions, and $h\nu$ denotes the photon energy. The E_d and E_o values of the samples were computed from the slope $(E_d/E_o)^{-1}$ and intercept (E_o/E_d) of Fig. 7. The obtained E_o and E_d values show the validity of the single-oscillator model for the nanolayers generated.

It is a known fact that there is a proportion of the polarizability of any solid material to the dielectric constant. This situation is associated with the intensity of the state within the forbidden energy gap. In this regard, it is crucial to investigate the real and imaginary parts of the complex dielectric constant. The definition of the dielectric constant is made as follows: $\epsilon = \epsilon_1 - i\epsilon_2$, i.e. ϵ_1, ϵ_2 are the real and imaginary parts of the complex dielectric constant, respectively. This is expressed by the following equation [35]:

$$\epsilon_1 = n^2 - k^2 \tag{8}$$

ve

$$\epsilon_2 = 2nk \tag{9}$$

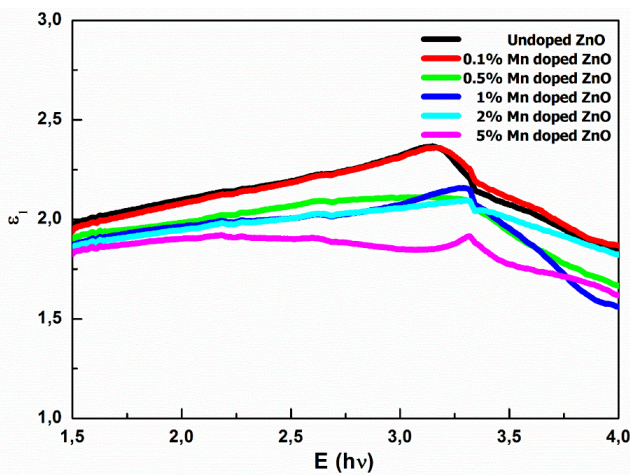


Figure 8. The plots of ϵ_1 -E Mn: ZnO nanolayers.

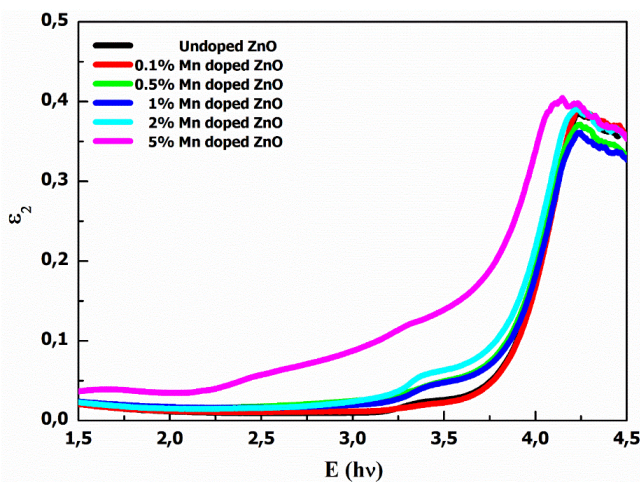


Figure 9. The plots of ϵ_2 -E Mn: ZnO nanolayers

Fig. 8 and Fig. 9 demonstrate the interconnection of the real and imaginary parts of the dielectric constant on the pho-

ton energy ($h\nu$), respectively. Figs. 8 and 9 showed the real and imaginary dielectric constant changes in the visible region for all nanostructured thin films. With increasing energy, an increase occurs in both the real and imaginary dielectric constant values of the nanolayers. The mentioned increase in optical conductivity is believed to result from electrons excited by photon energy [36]. The graph in Fig. 9 showed a peak reflecting the general band structure. The presence of the mentioned peak results from the photo-excitation process when electrons are excited from the valence band to the conduction band [21]. The real and imaginary dielectric constant of the films changed due to the effect of Mn-doping. Furthermore, the average ϵ_1 values are observed to be higher than ϵ_2 in the studied samples. There is an association of the mentioned difference between the real and imaginary parts of optical conductivity with the densities of state (DOS) of the films in the energy band ranges.

3.2. Non-linear optical properties of nanostructured pure and Mn-doped ZnO films

The effect of light on nanomaterials plays an essential role in different optical device applications because of the high non-linear precision. When high radiation intensity occurs in the material, such as laser, it produces non-linear effects such as second ($\chi^{(2)}$) and sensitivity ($\chi^{(3)}$). This is caused by the interaction of induced polarization (P) with the applied electric field (E). These non-linear sensitivities allow us to obtain information about samples that will resist high laser pulses during second and third-order impacts. In the literature, several methods are used to calculate the nonlinear refractive index and optical polarization. However, the ideal equations for thin films are expressed below [37]:

$$p = \chi^{(1)}E + P_{NL} \tag{10}$$

Where;

$$P_{NL} = \chi^{(2)}E^2 + \chi^{(3)}E^3 \tag{11}$$

and ($\chi^{(1)}$) refers to the linear optical susceptibility, and the other parameters are the same as the mentioned above. In the same manner, the linear refractive index $n(\lambda)$ is expressed by the following equation:

$$n(\lambda) = n_0(\lambda) + n_2(E)^2 \tag{12}$$

here $n(\lambda)$ is defined as $n_0(\lambda) \gg n_2(\lambda)$, $n(\lambda) = n_0(\lambda)$, and (E^2) denotes the mean square values of the electric field. It is possible to calculate ($\chi^{(1)}$) using the relation presented below:

$$\chi^{(1)} = (n^2 - 1)/4\pi \tag{13}$$

The ($\chi^{(3)}$) value can be calculated as follows:

$$\chi^{(3)} = A[(\chi^{(1)})^4] \tag{14}$$

Using Eqs. (13) and (14), the following equation is obtained:

$$\chi^{(3)} = \frac{A}{(4\pi)^4} (n^2 - 1)^4 \tag{15}$$

where A refers to a constant, and its value is 1.7×10^{-10} esu. It is possible to describe the non-linear refractive index from the relation presented below:

$$n_2 = \frac{12\pi\chi^{(3)}}{n_0^3} \tag{16}$$

The variations of linear, third-order susceptibilities and nonlinear refractive index with the wavelength of pure and Mn-doped ZnO thin films were demonstrated in Fig. 10, Fig. 11, and Fig. 12, respectively.

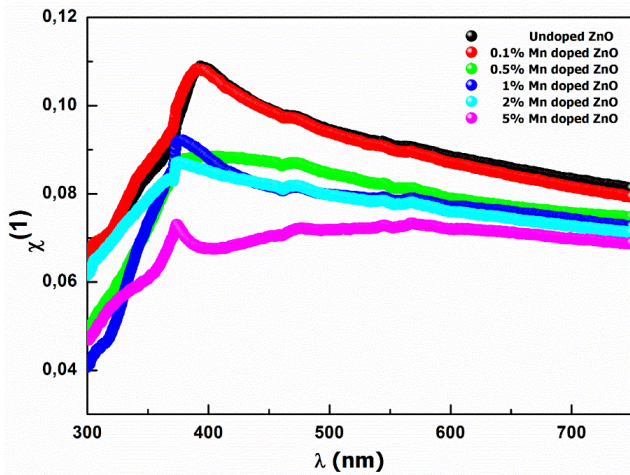


Figure 10. Linear optical susceptibility of the Mn: ZnO nanolayers.

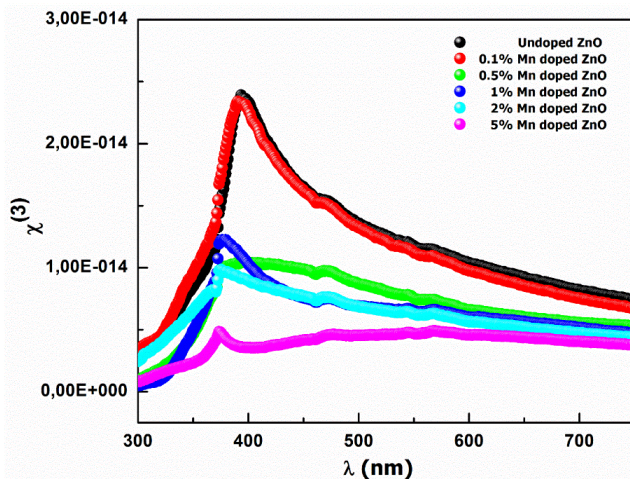


Figure 11. Third-order nonlinear optical susceptibility of the Mn: ZnO nanolayers.

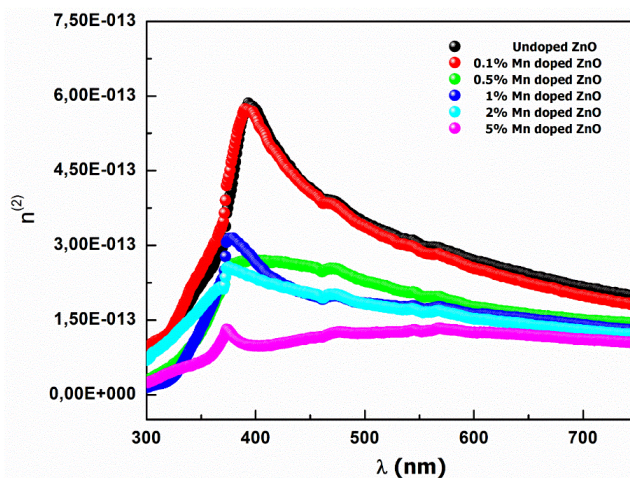


Figure 12. The nonlinear refractive index of the Mn: ZnO nanolayers.

From the obtained graphs, it is clearly seen that linear and non-linear sensitivities increase with wavelength and are saturated at certain wavelengths. This type of behavior is

usually due to the regularity of atoms in materials with high levels of crystallization [6]. The behavior in question has been explained by the enhancement in the crystallinity of the pure zinc oxide due to the Mn doping concentration and the high polarization of the doped samples compared to the pure material. Therefore, the susceptibilities of doped samples increase as the level of crystallization increases due to the increased doping concentration. The linear susceptibilities in the current calculations vary between 0.04 and 0.11, while nonlinear susceptibilities vary between 1.05×10^{-14} and 9.41×10^{-15} esu, which demonstrates the impact of doping in ZnO thin films. The calculated optical parameters were compared with previous studies of zinc oxide and results are shown in Table 3.

Table 3. Nonlinear optical parameters of present work on prepared Mn: ZnO nanolayers

Samples	$\chi^{(3)}$ (esu)	$n^{(2)}$ (esu)
Pure ZnO	2.41×10^{-14}	5.96×10^{-13}
0.1% Mn doped ZnO	2.32×10^{-14}	5.82×10^{-13}
0.5 % Mn doped ZnO	1.05×10^{-14}	2.73×10^{-13}
1 % Mn doped ZnO	1.25×10^{-14}	3.22×10^{-13}
2 % Mn doped ZnO	9.41×10^{-15}	2.62×10^{-13}
5 % Mn doped ZnO	5.17×10^{-15}	1.36×10^{-13}

These values show that prepared samples are higher than the values of ZnO thin films studied before and Mn has a significant impact on ZnO thin films and gives better results for nonlinear optical applications. Therefore, prepared Mn-doped ZnO thin films in many applications can be used in place of other metal oxide thin films.

4. CONCLUSION

Mn: ZnO thin films were successfully produced with the sol-gel spin coating technique, a simple and effective method. The impact of Mn doping concentration on the optical characteristics was discussed in detail. The optical characteristics of films state that Mn^{2+} ions substitute for the Zn^{2+} ion without altering the wurtzite structure of ZnO. The results indicate that the average values of optical transmission of the samples are greater than 80% and that these materials can be used in optical devices. It was found out that mainly grain size, density, and Mn concentration determine the refractive index of Mn-doped ZnO thin films. The decreasing optical bandgap of the samples with Mn doping is usually caused by the sp-d exchange interaction. All of these cases show that different concentrations of Mn doping cause some levels of impurities or have some effect on the existing levels and thus affect the type of transition. All these data confirm that Mn doping alters both opto-electrical and nonlinear optical properties.

5. REFERENCES

- [1] Akcan, D., Gungor, A., Arda, L. (2018). Structural and optical properties of Na-doped ZnO films. *Journal of Molecular Structure*, 1161: 299–305. doi:10.1016/j.molstruc.2018.02.058
- [2] Aydin, H., El-Nasser, H. M., Aydin, C., Al-Ghamdi, A. A., Yakuphanoglu, F. (2015). Synthesis and characterization of nanostructured

- undoped and Sn-doped ZnO thin films via sol-gel approach. *Applied Surface Science*, 350: 109–114. doi:10.1016/j.apsusc.2015.02.189
- [3] Aydin, H., Yakuphanoglu, F., Aydin, C. (2019). Al-doped ZnO as a multifunctional nanomaterial: Structural, morphological, optical and low-temperature gas sensing properties. *Journal of Alloys and Compounds*, 773: 802–811. doi:10.1016/j.jallcom.2018.09.327
- [4] Aydin, C., Abd El-sadek, M. S., Zheng, K., Yahia, I. S., Yakuphanoglu, F. (2013). Synthesis, diffused reflectance and electrical properties of nanocrystalline Fe-doped ZnO via sol-gel calcination technique. *Optics & Laser Technology*, 48: 447–452. doi:10.1016/j.optlas-tec.2012.11.004
- [5] Aydin, C. (2018). The functionalization of morphological, structural and optical properties of Fe doped SnO₂ nanocrystals synthesized by the sol-gel method. *Journal of Materials Science: Materials in Electronics*, 29(23): 20087–20096. doi:10.1007/s10854-018-0140-8
- [6] Aydin, C., Benhaliliba, M., Al-Ghamdi, A. A., Gafer, Z. H., El-Tantawy, F., Yakuphanoglu, F. (2013). Determination of optical band gap of ZnO:ZnAl₂O₄ composite semiconductor nanopowder materials by optical reflectance method. *Journal of Electroceramics*, 31(1-2): 265–270. doi:10.1007/s10832-013-9829-5
- [7] Akcan, D., Ozharar, S., Ozugurlu, E., Arda, L. (2019). The effects of Co/Cu Co-doped ZnO thin films: An optical study. *Journal of Alloys and Compounds*, 797: 253–261. doi:10.1016/j.jallcom.2019.05.126
- [8] Aksoy, S., Caglar, Y. (2019). Synthesis of Mn doped ZnO nanopowders by MW-HTS and its structural, morphological and optical characteristics. *Journal of Alloys and Compounds*, 781: 929–935. doi:10.1016/j.jallcom.2018.12.101
- [9] Aydin, C. (2019). Synthesis of Pd:ZnO nanofibers and their optical characterization dependent on modified morphological properties. *Journal of Alloys and Compounds*, 777: 145–151. doi:10.1016/j.jallcom.2018.10.325
- [10] Aydin, H., Aydin, C., Al-Ghamdi, A. A., Farooq, W. A., Yakuphanoglu, F. (2016). Refractive index dispersion properties of Cr-doped ZnO thin films by sol-gel spin coating method. *Optik*, 127(4): 1879–1883. doi:10.1016/j.ijleo.2015.10.230
- [11] Aydin, H., Gündüz, B., Aydin, C. (2019). Surface morphology, spectroscopy, optical and conductivity properties of transparent poly(9-vinylcarbazole) thin films modified with graphene oxide. *Synthetic Metals*, 252: 1–7. doi:10.1016/j.synthmet.2019.04.002
- [12] Aydin, H., Mansour, S. A., Aydin, C., Al-Ghamdi, A. A., Al-Hartomy, O. A., El-Tantawy, F., Yakuphanoglu, F. (2012). Optical properties of nanostructure boron doped NiO thin films. *Journal of Sol-Gel Science and Technology*, 64(3): 728–733. doi:10.1007/s10971-012-2909-1
- [13] Caglar, M., Ilcan, S., Caglar, Y., Yakuphanoglu, F. (2009). Electrical conductivity and optical properties of ZnO nanostructured thin film. *Applied Surface Science*, 255(8): 4491–4496. doi:10.1016/j.apsusc.2008.11.055
- [14] Caglar, Y. (2013). Sol-gel derived nanostructure undoped and cobalt doped ZnO: Structural, optical and electrical studies. *Journal of Alloys and Compounds*, 560: 181–188. doi:10.1016/j.jallcom.2013.01.080
- [15] Caglar, Y., Ilcan, S., Caglar, M., Yakuphanoglu, F. (2007). Effects of In, Al and Sn dopants on the structural and optical properties of ZnO thin films. *Spectrochimica Acta Part A: Molecular and Biomolecular Spectroscopy*, 67(3-4): 1113–1119. doi:10.1016/j.saa.2006.09.035
- [16] Shinde, V. R., Gujar, T. P., Lokhande, C. D., Mane, R. S., Han, S.-H. (2006). Mn doped and undoped ZnO films: A comparative structural, optical and electrical properties study. *Materials Chemistry and Physics*, 96(2-3): 326–330. doi:10.1016/j.matchemphys.2005.07.045
- [17] Chaitra, U., Kekuda, D., Mohan Rao, K. (2017). Effect of annealing temperature on the evolution of structural, microstructural, and optical properties of spin coated ZnO thin films. *Ceramics International*, 43(9): 7115–7122. doi:10.1016/j.ceramint.2017.02.144
- [18] Ganesh, V., Salem, G. F., Yahia, I. S., Yakuphanoglu, F. (2017). Synthesis, Optical and Photoluminescence Properties of Cu-Doped ZnO Nano-Fibers Thin Films: Nonlinear Optics. *Journal of Electronic Materials*, 47(3): 1798–1805. doi:10.1007/s11664-017-5950-6
- [19] Hu, D., Liu, X., Deng, S., Liu, Y., Feng, Z., Han, B., ... Wang, Y. (2014). Structural and optical properties of Mn-doped ZnO nanocrystalline thin films with the different dopant concentrations. *Physica E: Low-Dimensional Systems and Nanostructures*, 61: 14–22. doi:10.1016/j.physe.2014.03.007
- [20] Islam, M. R., Rahman, M., Farhad, S. F. U., Podder, J. (2019). Structural, optical and photocatalysis properties of sol-gel deposited Al-doped ZnO thin films. *Surfaces and Interfaces*, 16: 120–126. doi:10.1016/j.surfin.2019.05.007
- [21] Jacob, A. A., Balakrishnan, L., Meher, S. R., Shambavi, K., Alex, Z. C. (2017). Structural, optical and photodetection characteristics of Cd alloyed ZnO thin film by spin coating. *Journal of Alloys and Compounds*, 695: 3753–3759. doi:10.1016/j.jallcom.2016.11.265
- [22] Karmakar, R., Neogi, S. K., Banerjee, A., Bandyopadhyay, S. (2012). Structural; morphological; optical and magnetic properties of Mn doped ferromagnetic ZnO thin film. *Applied Surface Science*, 263: 671–677. doi:10.1016/j.apsusc.2012.09.133
- [23] Kaur, G., Mitra, A., Yadav, K. L. (2015). Pulsed laser deposited Al-doped ZnO thin films for optical applications. *Progress in Natural Science: Materials International*, 25(1): 12–21. doi:10.1016/j.pnsc.2015.01.012
- [24] Mia, M. N. H., Pervez, M. F., Hossain, M. K., Reefaz Rahman, M., Uddin, M. J., Al Mashud, M. A., ... Hoq, M. (2017). Influence of Mg content on tailoring optical bandgap of Mg-doped ZnO thin film prepared by sol-gel method. *Results in Physics*, 7: 2683–2691. doi:10.1016/j.rinp.2017.07.047
- [25] Sankar Ganesh, R., Durgadevi, E., Navaneethan, M., Patil, V. L., Pon-nusamy, S., Muthamizhchelvan, C., ... Hayakawa, Y. (2017). Low temperature ammonia gas sensor based on Mn-doped ZnO nanoparticle decorated microspheres. *Journal of Alloys and Compounds*, 721: 182–190. doi:10.1016/j.jallcom.2017.05.315
- [26] Aydin, H. (2014). Electrical and Optical Properties of Titanium Dioxide-Carbon Nanotube Nanocomposites. *Journal of Nanoelectronics and Optoelectronics*, 9(5): 608–613. doi:10.1166/jno.2014.1642
- [27] Shukla, P., Tiwari, S., Joshi, S. R., Akshay, V. R., Vasundhara, M., Varma, S., ... Chanda, A. (2018). Investigation on structural, morphological and optical properties of Co-doped ZnO thin films. *Physica B: Condensed Matter*, 550: 303–310. doi:10.1016/j.physb.2018.08.046
- [28] Sindhu, H. S., Maidur, S. R., Patil, P. S., Choudhary, R. J., Rajendra, B. V. (2019). Nonlinear optical and optical power limiting studies of Zn_{1-x}Mn_xO thin films prepared by spray pyrolysis. *Optik*, 182: 671–681. doi:10.1016/j.ijleo.2019.01.031
- [29] Singh, P., Kaushal, A., Kaur, D. (2009). Mn-doped ZnO nanocrystalline thin films prepared by ultrasonic spray pyrolysis. *Journal of Alloys and Compounds*, 471(1-2): 11–15. doi:10.1016/j.jallcom.2008.03.123
- [30] Sivalingam, D., Gopalakrishnan, J. B., Rayappan, J. B. B. (2012). Structural, morphological, electrical and vapour sensing properties of Mn doped nanostructured ZnO thin films. *Sensors and Actuators B: Chemical*, 166-167, 624–631. doi:10.1016/j.snb.2012.03.023

- [31] Srinivasan, G., Kumar, J. (2008). Effect of Mn doping on the microstructures and optical properties of sol-gel derived ZnO thin films. *Journal of Crystal Growth*, 310(7-9): 1841–1846. doi:10.1016/j.jcrysgro.2007.10.056
- [32] Ton-That, C., Foley, M., Phillips, M. R., Tsuzuki, T., Smith, Z. (2012). Correlation between the structural and optical properties of Mn-doped ZnO nanoparticles. *Journal of Alloys and Compounds*, 522: 114–117. doi:10.1016/j.jallcom.2012.01.116
- [33] Vijayaprasath, G., Murugan, R., Ravi, G., Mahalingam, T., Hayakawa, Y. (2014). Characterization of dilute magnetic semiconducting transition metal doped ZnO thin films by sol-gel spin coating method. *Applied Surface Science*, 313: 870–876. doi:10.1016/j.apsusc.2014.06.093
- [34] Xin, M., Hu, L. Z., Liu, D.-P., Yu, N.-S. (2014). Effect of Mn doping on the optical, structural and photoluminescence properties of nanostructured ZnO thin film synthesized by sol-gel technique. *Superlattices and Microstructures*, 74: 234–241. doi:10.1016/j.spmi.2014.06.009
- [35] Yang, S., Zhang, Y. (2013). Structural, optical and magnetic properties of Mn-doped ZnO thin films prepared by sol-gel method. *Journal of Magnetism and Magnetic Materials*, 334: 52–58. doi:10.1016/j.jmmm.2013.01.026
- [36] Zhong, J. bo, Li, J. zhang, He, X. yang, Zeng, J., Lu, Y., Hu, W., Lin, K. (2012). Improved photocatalytic performance of Pd-doped ZnO. *Current Applied Physics*, 12(3): 998–1001. doi:10.1016/j.cap.2012.01.003
- [37] Jilani, A., Abdel-wahab, M. S., Al-ghamdi Attieh A., Dahlan, A. sadik, Yahia, I. S. (2016). Nonlinear optical parameters of nanocrystalline AZO thin film measured at different substrate temperatures. *Physica B: Condensed Matter*, 481: 97–103. doi:10.1016/j.physb.2015.10.038